

# Redox-dependent dimerization of p38 $\alpha$ mitogen-activated protein kinase with mitogen-activated protein kinase kinase 3

Received for publication, March 10, 2017, and in revised form, July 13, 2017. Published, Papers in Press, July 24, 2017, DOI 10.1074/jbc.M117.785410

Rekha Bassi, Joseph R. Burgoyne, Gian F. DeNicola, Olena Rudyk, Vittorio DeSantis, Rebecca L. Charles, Philip Eaton, and Michael S. Marber<sup>1</sup>

From the King's College London British Heart Foundation Centre of Excellence, Department of Cardiology, The Rayne Institute, St. Thomas' Hospital, London SE1 7EH, United Kingdom

Edited by Alex Tokor

The kinase p38 $\alpha$  MAPK (p38 $\alpha$ ) plays a pivotal role in many biological processes. p38 $\alpha$  is activated by canonical upstream kinases that phosphorylate the activation region. The purpose of our study was to determine whether such activation may depend on redox-sensing cysteines within p38 $\alpha$ . p38 $\alpha$  was activated and formed a disulfide-bound heterodimer with MAP2K3 (MKK3) in rat cardiomyocytes and isolated hearts exposed to H<sub>2</sub>O<sub>2</sub>. This disulfide heterodimer was sensitive to reduction by mercaptoethanol and was enhanced by the thioredoxin-reductase inhibitor auranofin. We predicted that Cys-119 or Cys-162 of p38 $\alpha$ , close to the known MKK3 docking domain, were relevant for these redox characteristics. The C119S mutation decreased whereas the C162S mutation increased the dimer formation, suggesting that these two Cys residues act as vicinal thiols, consistent with C119S/C162S being incapable of sensing H<sub>2</sub>O<sub>2</sub>. Similarly, disulfide heterodimer formation was abolished in H9C2 cells expressing both MKK3 and p38 $\alpha$  C119S/C162S and subjected to simulated ischemia and reperfusion. However, the p38 $\alpha$  C119S/C162S mutants did not exhibit appreciable alteration in activating dual phosphorylation. In contrast, the anti-inflammatory agent 10-nitro-oleic acid (NO<sub>2</sub>-OA), a component of the Mediterranean diet, reduced p38 $\alpha$  activation and covalently modified Cys-119/Cys-162, probably obstructing MKK3 access. Moreover, NO<sub>2</sub>-OA reduced the dephosphorylation of p38 $\alpha$  by hematopoietic tyrosine phosphatase (HePTP). Furthermore, steric obstruction of Cys-119/Cys-162 by NO<sub>2</sub>-OA pretreatment in Langendorff-perfused murine hearts prevented the p38-MKK3 disulfide dimer formation and attenuated H<sub>2</sub>O<sub>2</sub>-induced contractile dysfunction. Our findings suggest that cysteine residues within p38 $\alpha$  act as redox sensors that can dynamically regulate the association between p38 and MKK3.

p38 MAPK (p38) family members coordinate, expand, and transmit intricate signals from cell surface receptors and other environmental cues. Like that of their counterparts ERK and JNK, p38 activation is classically orchestrated through a three-step cascade made up of the MAPK, another upstream MAPK kinase (MAPKK/MKK/MEK), and another, further upstream MAPKK kinase (MAPKKK or MEKK) (1). All four p38 MAPK isoforms,  $\alpha$ ,  $\beta$ ,  $\gamma$ , and  $\delta$ , share significant sequence homology (2) but differ in their expression patterns, activation profiles, and substrates, suggesting divergent cellular functions. p38 $\alpha$  is ubiquitously expressed and is the only isoform essential for development, because its absence results in embryonic lethality (3). Consequently, it is the most widely studied isoform, implicated in numerous biological and pathological processes.

p38 $\alpha$  interfaces with a diverse set of partners, including upstream activators, deactivating phosphatases, and substrates. To confer fidelity and regulate the extensive input signals to the appropriate cellular outcomes, p38 $\alpha$ , like all other MAPKs, uses a docking strategy to specifically bind to its interacting partners. Linear sequence motifs are employed within interacting partners that recognize features on p38 $\alpha$  remote from the kinase active site. Of these, the most ubiquitous are the D-motifs (4). Crystallographic studies, together with mutagenic analyses of docking interactions of p38 $\alpha$ , have revealed that the D-motif-binding site is formed of short peptide sequences composed of two subsites, recognizing an acidic patch (CD domain) and a hydrophobic docking groove (5, 6). Interestingly, the p38 $\alpha$  substrate and upstream activators, MEF2a and MKK3b, respectively, were reported to interact with p38 $\alpha$  at the D-motif-binding site (7). They both appeared to engage the hydrophobic docking groove and induced similar local but different distant conformational changes within p38 $\alpha$ . Pertinent to this, more recent crystallographic data of p38 $\alpha$  bound to a peptide derived from MKK3b (containing the D-motif consensus sequence) induced a third conformation, distinct from unphosphorylated and phosphorylated p38 $\alpha$  (8). The exact mode by which a protein partner binds the common docking site on p38 $\alpha$  can therefore have profound consequences on the structure and presumably the function of p38 $\alpha$ .

This work was supported by British Heart Foundation Grant SP/14/2/30922 and Medical Research Council Grant MR/J007501/1. This work was also supported by the Department of Health via the National Institute for Health Research (NIHR) comprehensive Biomedical Research Centre and Clinical Research Facilities awards to Guy and St. Thomas NHS Foundation Trust in partnership with King's College London and King's College Hospital NHS Foundation Trust. The authors declare that they have no conflicts of interest with the contents of this article.

✂ Author's Choice—Final version free via Creative Commons CC-BY license.

<sup>1</sup> To whom correspondence should be addressed: Cardiovascular Division, KCL, Rayne Institute, St. Thomas' Hospital Campus, London SE1 7EH, United Kingdom. Tel.: 44-20-7188-1008; Fax: 44-20-7188-0970; E-mail: mike.marber@kcl.ac.uk.

## p38 $\alpha$ -MKK3 dimerization

The oxidation of protein cysteine residues has emerged as an important means of regulating protein kinase function. This form of protein regulation is elicited by an imbalanced cellular redox state due to changes in reactive oxygen or nitrogen species formation or alterations in the cellular antioxidant or reducing system (9). The redox sensitivity of a protein cysteine residue is very dependent on its precise surrounding microenvironment. Those cysteines with a low  $pK_a$ , due to the presence of neighboring basic amino acids lysine, arginine, or histidine, tend to be reactive with oxidants because they are readily deprotonated. Low  $pK_a$  thiols exist as a thiolate anion ( $S^-$ ) at neutral cellular pH, making them more reactive with electrophilic oxidants compared with those in the protonated thiol state (10). A reactive thiol can undergo a diverse range of oxidative modifications that is dependent on the oxidant species present. Because p38 $\alpha$  is activated by oxidative stress, we hypothesized that this could be mediated through direct thiol oxidation. Certainly, this is consistent with the major upstream p38 $\alpha$  kinase, MKK3, having a cysteine adjacent to its D-motif that forms an intermolecular disulfide with p38 $\alpha$  when cocrystallized (8). Here, we investigated whether redox-sensitive cysteines in p38 $\alpha$  MAPK influence its activation during oxidant stress.

## Results

### Oxidants induce reversible higher-molecular weight forms of p38 and MKK3

Exposure of adult rat ventricular myocyte (AVRMs)<sup>2</sup> to  $H_2O_2$ , peroxyxynitrite, SIN-1, or diamide, oxidants previously described as inducing activation of p38, revealed the existence of both monomeric and multimeric species of p38 by immunoblot analysis following SDS-PAGE under non-reducing conditions (Fig. 1A). The majority of p38 was detected as a band that resolved at the expected relative molecular mass of  $\sim 40$  kDa. We observed that p38 not only became phosphorylated following exposure to  $100 \mu M H_2O_2$ ,  $500 \mu M ONOO^-$ ,  $200 \mu M SIN-1$ , or  $50 \mu M$  diamide, as expected, but these also induced the appearance of phospho-p38 $\alpha$  migrating at a higher apparent molecular mass between 70 and 100 kDa (Fig. 1A). Analysis of these cell lysates also revealed activation of MKK3, the prototypical upstream kinase activator of p38, under identical conditions. Similar to p38, MKK3 was present in both monomeric and multimeric forms. To demonstrate that the formation of oxidant-mediated multimers was due to disulfide bond formation, the complexes were first isolated from a non-reducing SDS-PAGE using the 70 and 100 kDa molecular mass markers as a guide to excise the relevant portion of the gel, indicated by *dashed frames* (see Fig. 1B). The portion of the gel containing the multimeric complexes was then overlaid onto a fresh SDS-polyacrylamide gel and resolved under reducing conditions, by the inclusion of 2-mercaptoethanol (Fig. 1B). Subsequent immunoblot analysis detected total p38 and MKK3 as bands now resolved at  $\sim 38$  kDa and the absence of multimeric forms, verifying that complexes contained MKK3 and p38 bound by reversible

disulfide bonds. The lack of p38 and MKK3 in the control lanes under reducing conditions demonstrates that they did not interact under basal conditions (non-oxidizing) and therefore did not form a higher-molecular weight complex and were absent from the portion of the gels indicated by the *dashed frame*.

### The p38 and MKK3 multimers are probably subject to continuous redox cycling

Because the oxidant-induced higher-molecular weight complexes containing p38 and MKK3 represented a very small portion of the total cellular p38/MKK3 protein, we wondered whether disulfide reductase enzymes (11), such as thioredoxin, were limiting multimer accumulation. Administration of  $2 \mu M$  auranofin, a thioredoxin-reductase inhibitor, for 30 min prior to the exposure to  $H_2O_2$  resulted in an accumulation of the p38- and MKK3-containing multimer (Fig. 1C). Auranofin was so effective in trapping the oxidized multimer that it could be detected at low concentrations and even in the absence of  $H_2O_2$ . These observations suggest that the p38/MKK3-containing multimers undergo continuous redox cycling within the cellular environment and can therefore be dynamically regulated by endogenous oxidant formation.

### $H_2O_2$ induces the formation p38 and MKK3 multimers in isolated rat hearts

We next examined rat hearts exposed to  $H_2O_2$  during aerobic perfusion to assess whether the  $H_2O_2$ -induced multimers that we observed in AVRMs also occurred in the more complex and physiological environment of the intact heart. We noticed that monomeric forms of both phosphorylated p38 and MKK3 were detected in hearts that underwent baseline aerobic perfusion, and multimeric forms appeared only upon exposure to  $H_2O_2$  in a dose-dependent manner (Fig. 1D). Monomeric bands are determined by the immunosignal that resolves at the apparent molecular mass of p38 and MKK3 ( $\sim 40$  kDa), according to the antibody supplier. p38 and MKK3 exist largely in monomeric form (reduced form). A small proportion becomes complexed following exposure to  $H_2O_2$ . Consequently, the monomer bands are overexposed. Nonetheless, the abundance of multimer relative to monomer seemed greater than in isolated cells, reinforcing potential pathophysiological relevance and encouraging further analysis.

### The p38- and MKK3-containing multimers are heterodimers

Observations so far indicate that oxidant-induced, high-molecular weight, disulfide-dependent, reversible aggregates form that contain MKK3 and p38 immunoreactivity. The apparent molecular weight suggests these are either disulfide-bound hetero- or homodimers. To discern between these possibilities, we expressed FLAG-tagged WT p38 $\alpha$  and HA-tagged MKK3 in HEK293 cells. Using both non-reducing and reducing SDS-PAGE immunoblot analysis of lysates of cells overexpressing p38 $\alpha$  and MKK3 in the absence or presence of  $H_2O_2$ , we were able to largely recapitulate the observations in AVRMs (Fig. 1, A–C), isolated heart preparations (Fig. 1D), and HEK293 cells (Fig. 2A). In the presence of  $H_2O_2$ , p38 $\alpha$  and MKK3 both became phosphorylated. Despite effective ectopic overexpression of these proteins, a higher-molecular weight complex was only seen when MKK3 and

<sup>2</sup> The abbreviations used are: AVRMs, adult rat ventricular myocyte; SI, simulated ischemia; dBBr, dibromobimane; HePTP, hematopoietic tyrosine phosphatase; ROS, reactive oxygen species; TCEP, tris(2-carboxyethyl)phosphine; ANOVA, analysis of variance; KHB, Krebs-Henseleit buffer; NO<sub>2</sub>-OA, 10-nitrooleic acid.

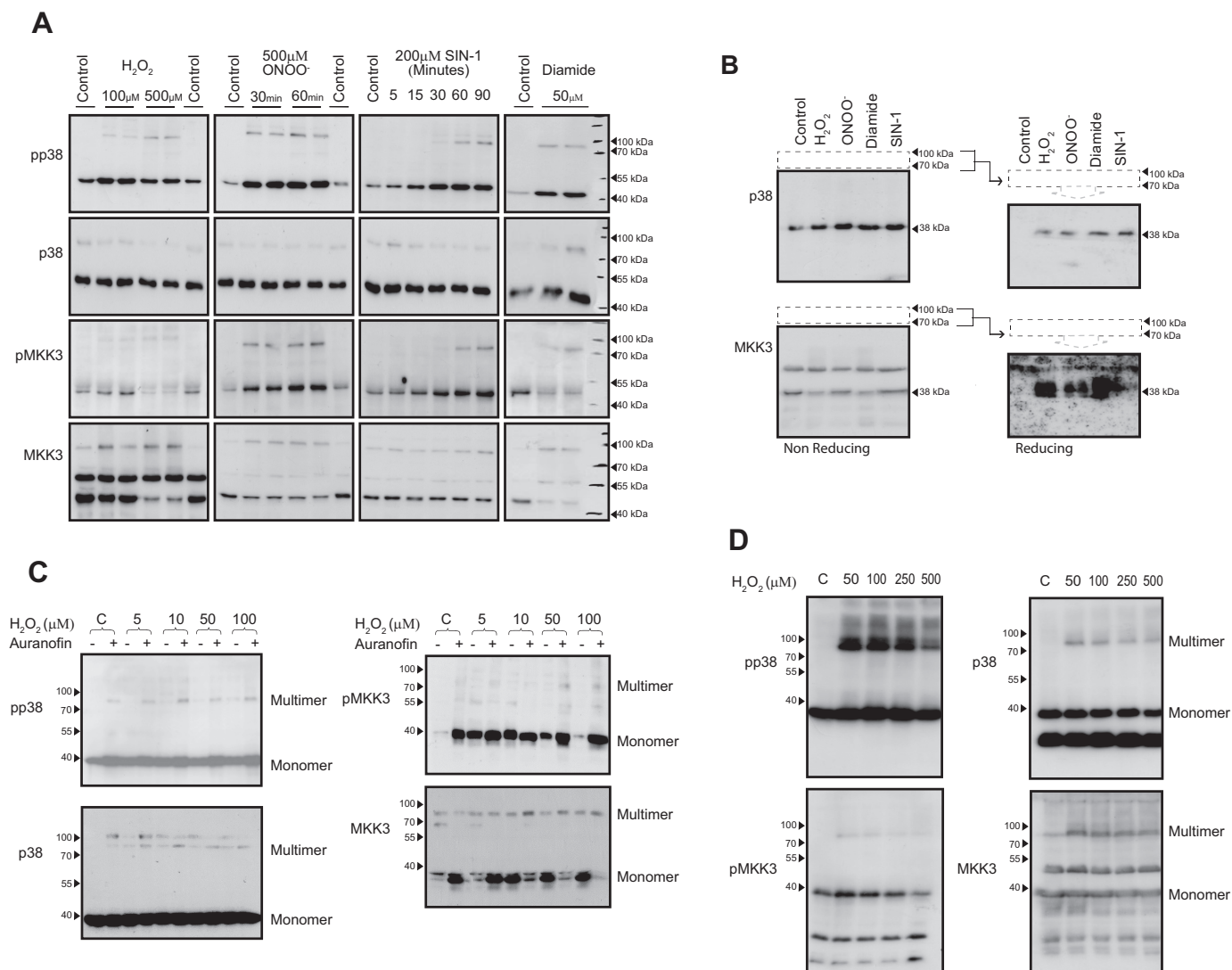


**Figure 1. Oxidants induce reversible higher molecular weight forms of p38 and MKK3 in rat myocardium.** *A*, non-reducing SDS-PAGE and immunoblot analysis of AVRM incubated with H<sub>2</sub>O<sub>2</sub>, ONOO<sup>-</sup>, SIN-1, or diamide. *B*, SDS-PAGE and immunoblot analysis of disulfide complexes (excised from non-reducing SDS-PAGE separation as in *A*) resolved under reducing conditions (by inclusion of 2-mercaptoethanol). *C*, non-reducing SDS-PAGE and immunoblot analysis of AVRM incubated with H<sub>2</sub>O<sub>2</sub> in the absence or presence of auranofin. The p38 and MKK3 multimers are subject to continuous cycling. *D*, non-reducing SDS-PAGE and immunoblot analysis of rat hearts exposed to H<sub>2</sub>O<sub>2</sub> during aerobic Langendorff perfusion. H<sub>2</sub>O<sub>2</sub> induces the formation p38 and MKK3 multimers in the intact heart in a manner similar to those seen in AVRM in *A*–*C*.

p38 $\alpha$  were co-expressed, suggesting that disulfide-bound homodimers do not form. These observations were verified using anti-FLAG and anti-HA antibodies (Fig. 2A). The administration of 2  $\mu$ M auranofin 30 min prior to exposure to H<sub>2</sub>O<sub>2</sub> in cells overexpressing both p38 $\alpha$  and MKK3 led to the accumulation of the disulfide dimer spontaneously and at low concentrations of H<sub>2</sub>O<sub>2</sub> (Fig. 2B), thus reinforcing the notion that the amount of oxidized p38 $\alpha$  that we observe is limited by the continued reductive action of endogenous thioredoxin.

#### Cysteines 119 and 162 of p38 $\alpha$ are involved in disulfide dimer formation

To further examine the formation of the H<sub>2</sub>O<sub>2</sub>-mediated heterodimer, we utilized a web-based program developed by Ricardo Sanchez and Jamil A. Momand (12) to predict which of the four cysteine residues of p38 $\alpha$  were likely to form disulfides. We entered published structural data deposited in the Protein

Data Bank (entry 1LEZ), describing the crystal structures of p38 $\alpha$  complexed to the docking sites on its nuclear substrate MEF2a and activator MKK3b (7). The results suggested that Cys-119 and Cys-162 could be potential disulfide-forming thiols located near the surface of the protein. Furthermore, the presence of neighboring lysine and histidine residues renders them more susceptible to electrophilic attack by lowering their  $pK_a$ . This, together with the observation that Cys-119 and Cys-162 may participate in hydrophobic contacts with the MAPK docking sites within MKK3b- and MEF2a-derived peptides (7), led us to substitute either or both of these residues with serine. We found that p38 $\alpha$ -cysteine mutants lacking either Cys-119, Cys-162, or both resulted in attenuation, enhancement, or abolition, respectively, of H<sub>2</sub>O<sub>2</sub>-mediated p38 $\alpha$ -MKK3 dimer formation (Fig. 2C). We believe that the formation of a reversible interdisulfide bond between p38 $\alpha$  and MKK3 occurs preferentially as a result of oxidation of the sulfhydryl group on Cys-119 by H<sub>2</sub>O<sub>2</sub>, because mutation of this residue attenuated the

## p38 $\alpha$ -MKK3 dimerization

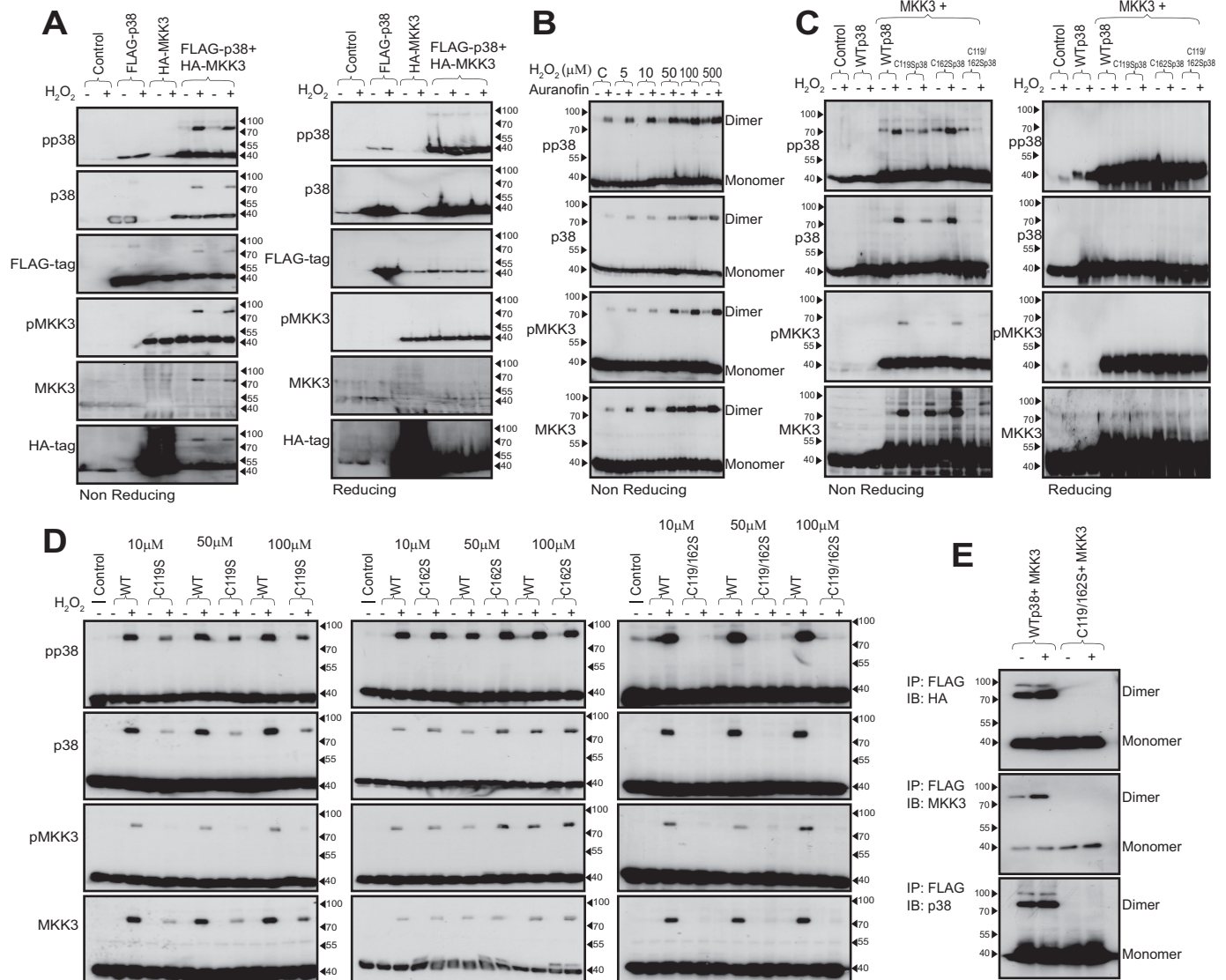


**Figure 2. The p38 and MKK3 containing multimers are heterodimers dependent on Cys-119 and Cys-162 of p38.** A, non-reducing and reducing SDS-PAGE and immunoblot analysis of HEK293 cells overexpressing FLAG-tagged WT p38 $\alpha$  and/or HA-tagged MKK3 in the presence or absence of 100  $\mu$ M H<sub>2</sub>O<sub>2</sub>. The anti-FLAG signal seen in the HA-MKK3 lanes is the result of "bleed-over" from neighboring lanes. B, non-reducing SDS-PAGE and immunoblot analysis of HEK293 cells overexpressing WT p38 $\alpha$  and MKK3 incubated with H<sub>2</sub>O<sub>2</sub> in the absence or presence of auranofin. The H<sub>2</sub>O<sub>2</sub>-mediated dimers are subject to continuous cycling. C, non-reducing and reducing SDS-PAGE and immunoblot analysis of HEK293 cells overexpressing WT p38 $\alpha$  or p38 $\alpha$ -cysteine mutants lacking either Cys-119, Cys-162, or both and treated with 100  $\mu$ M H<sub>2</sub>O<sub>2</sub>. Cysteines 119 and 162 of p38 $\alpha$  are both involved in disulfide dimer formation, but abundance is more dependent on Cys-119. D, non-reducing SDS-PAGE and immunoblot analysis of HEK293 cells overexpressing WT p38 $\alpha$  or p38 $\alpha$ -cysteine mutants and treatment with 10, 50, or 100  $\mu$ M H<sub>2</sub>O<sub>2</sub>. MKK3 and p38 $\alpha$  form a heterodimer dependent on Cys-119 and Cys-162. E, non-reducing SDS-PAGE and immunoblot analysis (IP) of HEK293 cells overexpressing WT p38 $\alpha$  or C119S/C162S p38 $\alpha$  and treated with 100  $\mu$ M H<sub>2</sub>O<sub>2</sub>, following FLAG immunoprecipitation (IP).

formation of the dimer. In contrast, cells containing intact Cys-119 but mutated Cys-162 (C162S) have a similar or greater abundance of the dimer (Fig. 2C). The double mutant (C119S/C162S) did not form any detectable dimer following treatment with 100  $\mu$ M H<sub>2</sub>O<sub>2</sub>. These differences in propensity to p38 $\alpha$ -MKK3 disulfide dimer formation between the cysteine mutants were verified on multiple repetitions and at lower, more physiological, concentrations of H<sub>2</sub>O<sub>2</sub> (see Fig. 2D). Furthermore, the presence and absence of dimer in immunoprecipitates from cells co-expressing FLAG-MKK3 and HA-WT p38 $\alpha$  or C119S/C162S p38 $\alpha$ , respectively, confirmed that MKK3 and p38 $\alpha$  form a disulfide-bound heterodimer dependent on these residues (Fig. 2E). Despite the abolition of disulfide dimerization with the C119S/C162S p38 $\alpha$  mutant, transphosphorylation of the p38 $\alpha$  activation loop by

MKK3 seems to proceed normally based on immunoreactivity of the monomeric form with anti-pTGpY dual phosphospecific antibody (Fig. 2, C and D). We therefore examined whether the ability to activate p38 $\alpha$  was disulfide dimer-dependent in another more pathophysiologically relevant cellular model.

### Simulated ischemia and reperfusion causes p38 $\alpha$ -MKK3 disulfide dimer formation dependent on Cys-119 and Cys-162 of p38 $\alpha$

We (13–15) and others (12, 16) have previously reported that p38 $\alpha$  becomes activated during myocardial ischemia and reperfusion. We investigated the role of dimer formation employing an *in vitro* model of simulated ischemia–reperfusion in a rat myoblast cell line (H9C2) that approximates the clinical setting

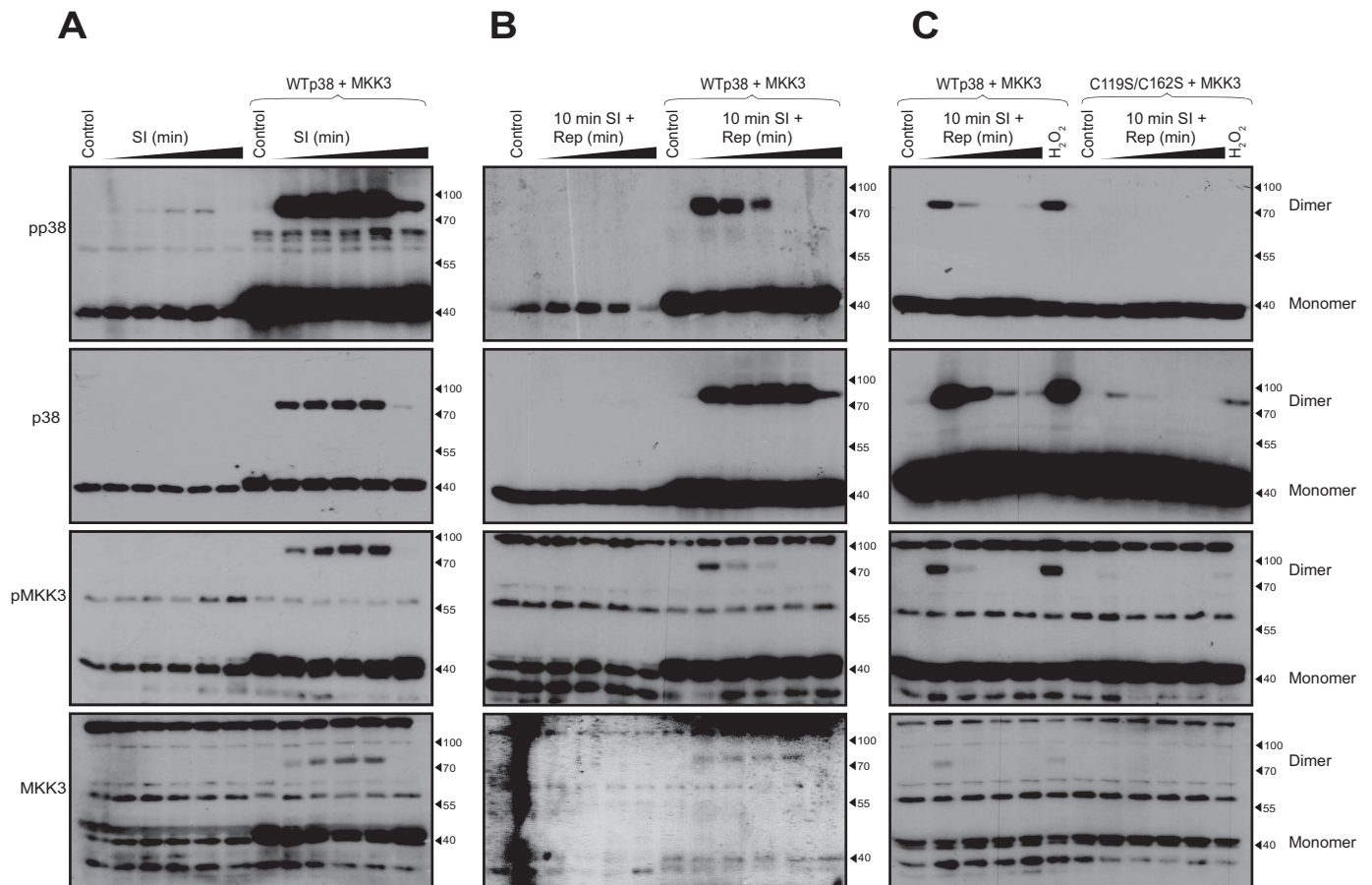


**Figure 3. Simulated ischemia and reperfusion causes p38 $\alpha$ -MKK3 disulfide dimer formation dependent on Cys-119 and Cys-162 of p38 $\alpha$ .** *A*, non-reducing SDS-PAGE and immunoblot analysis of H9C2 cells expressing endogenous or exogenous WT p38 $\alpha$  and MKK3 subjected to 5, 10, 20, or 40 min of simulated ischemia. *B*, non-reducing SDS-PAGE and immunoblot analysis of H9C2 cells expressing endogenous or exogenous WT p38 $\alpha$  and MKK3 subjected to 5, 10, 20, or 40 min of simulated ischemia, followed by 2.5, 5, 10, 20, or 40 min of simulated reperfusion. *C*, non-reducing SDS-PAGE and immunoblot analysis of H9C2 cells overexpressing WT p38 $\alpha$  or C119S/C162S p38 $\alpha$  and MKK3, subjected to 10 min of simulated ischemia and 2.5, 5, 10, 20, or 40 min of reperfusion.

of acute myocardial infarction (13). Exposure of native and transfected H9C2 cells to simulated ischemia (SI) led to p38 phosphorylation and formation of the p38 $\alpha$ -MKK3 disulfide dimer (Fig. 3A), mimicking the effect of H<sub>2</sub>O<sub>2</sub>. The phosphorylation of monomeric p38 $\alpha$  and MKK3 occurred in a time-dependent manner. The disulfide dimer was detectable after 5 min of SI, continued to increase until 20 min, and diminished to baseline after 40 min of SI. These observations were replicated in cells overexpressing p38 $\alpha$  and MKK3, albeit with a marked increase in p38 $\alpha$  activation compared with untransfected cells. The level of disulfide dimer formed during SI was notably higher than with 500  $\mu$ M H<sub>2</sub>O<sub>2</sub>. To investigate the effect of simulated reperfusion on the disulfide dimer formation, we subjected cells to 10 min of SI and increasing durations of reperfusion. As expected, disulfide dimer was detected in cells following 10 min of SI, with phosphorylation of both p38 $\alpha$  and MKK3. The disulfide dimer was also detected in cells following all of the durations of reperfusion that we tested. The phosphorylation of p38 $\alpha$  and MKK3 within the disulfide dimer was most marked at the 2.5- and 5-min time points of reperfusion (Fig. 3B). Identical experiments carried out on cells expressing the double cysteine mutant of p38 $\alpha$  confirmed that disulfide dimers were dependent on Cys-119/162, but the presence or absence of disulfide dimers did not appreciably alter dual phos-

phorylation of p38 $\alpha$  (Fig. 3C). Thus, in keeping with the results in HEK293 cells (see Fig. 2, C and D), abolishing disulfide dimer formation does not seem to impact p38 activation as assessed by dual phosphorylation of monomeric p38. We therefore examined further biochemical detail of the relevant cysteines to determine whether they can form adducts with small molecules that could sterically hinder recognition of MKK3 by p38 $\alpha$ .

#### ***Dibromobimane (dBBr) specifically reacts with closely spaced cysteine sulfhydryl groups***

The divergent effects of C119S and C162S on dimer formation (Fig. 2, C and D) suggest that they could be acting as vicinal thiols that are asymmetrically coupled. To determine the distance between Cys-119 and Cys-162, we exposed WT p38 $\alpha$  to dBBr, which emits at 477 nm when both of its alkylating groups, separated by 3–6 Å, become covalently linked to available reactive thiols. Incubation of WT p38 $\alpha$  with dBBr alone resulted in a significant increase in fluorescence, compared with the dBBr and tris(2-carboxyethyl)phosphine (TCEP) controls (Fig. 4A). The inclusion of 500  $\mu$ M H<sub>2</sub>O<sub>2</sub> led to a marked reduction of fluorescence, indicating that redox-sensitive cysteines had been oxidized and were unable to react with the dBBr. Preincubation of p38 $\alpha$  with diamide completely abolished the fluorescence signal with dBBr, confirming that the

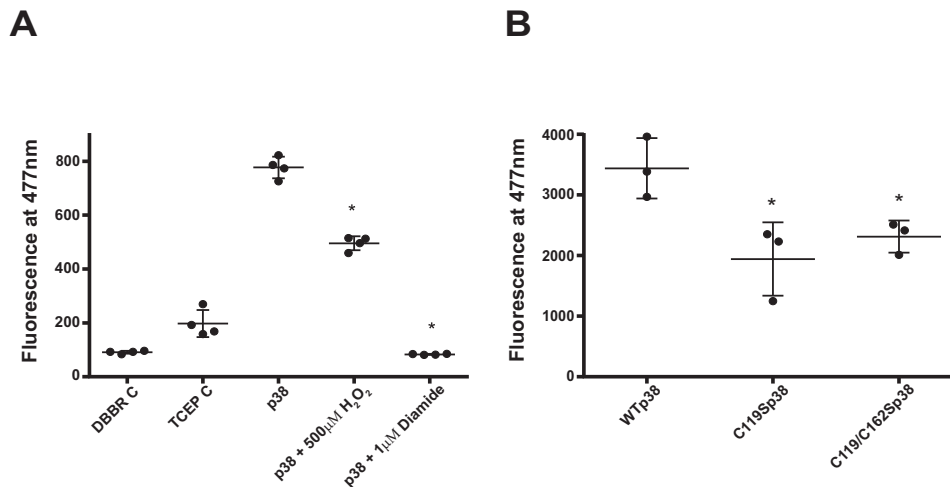


**Figure 4. dBBR reacts with wild-type and mutated p38 $\alpha$ .** A, dBBR fluorescence measurements from three separate experiments of WT p38 $\alpha$  incubated with dBBR, in the absence and presence of 500  $\mu$ M H<sub>2</sub>O<sub>2</sub> or 1  $\mu$ M diamide. Quantification data are shown as mean  $\pm$  S.E. (error bars). \*,  $p < 0.05$  versus p38, by one-way ANOVA and Tukey's test. B, dBBR fluorescence measurements from three separate experiments of WT p38 $\alpha$ , C119 p38 $\alpha$ , or C119S/C162S p38 $\alpha$  incubated with dBBR. Quantification data are shown as mean  $\pm$  S.D. (error bars). \*,  $p < 0.05$  versus WT p38 $\alpha$ , by one-way ANOVA and Newman–Keuls test.

signals observed were a result of dBBR-specific cross-linking vicinal thiols within p38 $\alpha$ .

In an attempt to verify our earlier observation that Cys-119 is the culpable thiol involved in the formation of an interdisulfide bond between p38 $\alpha$  and MKK3, we treated recombinant WT p38 $\alpha$  or the C119S p38 $\alpha$  mutant with dBBR. Incubation of the C119S p38 $\alpha$  mutant with dBBR resulted in a marked reduction of fluorescence emitted compared with WT p38 $\alpha$  (Fig. 4B). We, however, had expected a much greater reduction, if not an absence of a fluorescence signal, because dBBR should not fluoresce in the presence of only one of the vicinal pair. Interestingly, incubation of dBBR with the double mutant also emitted a respectable fluorescence signal that was comparable with that observed with C119S. These findings suggest that the signal observed with the cysteine mutants may represent “background” fluorescence resulting from adduction by dBBR of thiols on adjacent p38 $\alpha$  molecules that have their probability of close proximity enhanced by the high molarity of p38 $\alpha$  used in the assay.

#### Cysteine adduction attenuates the activation of p38 by MKK3

To investigate the biochemical significance of p38-MKK3 dimerization, we examined the activity of p38 $\alpha$  and C119S/C162S p38 $\alpha$  by performing *in vitro* kinase assays in the presence of 10-nitro-oleic acid (NO<sub>2</sub>-OA), an endogenous electrophilic lipid. NO<sub>2</sub>-OA has been reported to post-translationally modify proteins on redox-sensitive cysteines via reversible Michael addition reactions (17). Based on the crystal structure of p38 $\alpha$  bound to MKK3b (7), we envisaged that cysteine adduction by NO<sub>2</sub>-OA could potentially sterically hinder access by MKK3b, thereby preventing heterodimer formation. Dual phosphorylation of the TGY activation motif of p38 $\alpha$  and phosphorylation of its downstream substrate, ATF-2, were used as readouts of p38 activity. In keeping with our earlier observation in cells, where the activity of p38 was not appreciably altered by the absence of the redox-sensitive cysteines (Figs. 2 (C and D) and 3C), both p38 $\alpha$  and C119S/C162S p38 $\alpha$  became phosphorylated and activated following 30-min incubation

with MKK3b (Fig. 5A). This confirms that disabling disulfide dimer formation does not diminish MKK3 access to and consequent dual phosphorylation of p38 $\alpha$ . Moreover, the presence of NO<sub>2</sub>-OA inhibited the activation of p38 $\alpha$  but also, to a lesser extent, C119S/C162S p38 $\alpha$ . NO<sub>2</sub>-OA inhibited the phosphorylation and activity of p38 $\alpha$  at low micromolar concentrations (1  $\mu$ M NO<sub>2</sub>-OA versus vehicle control), whereas a 5-fold higher concentration of NO<sub>2</sub>-OA (5  $\mu$ M versus vehicle control) was required to achieve comparable inhibition of C119S/C162S p38 $\alpha$ . The diminished sensitivity of C119S/C162S p38 $\alpha$  suggests that NO<sub>2</sub>-OA selectively targets these redox-sensitive cysteines. We further interrogated this concept by examining the effect of NO<sub>2</sub>-OA on the activity of hematopoietic tyrosine phosphatase (HePTP), a member of a small family of phosphatases that specifically dephosphorylates p38. Like MKK3b and MEF2a, HePTP also interacts with the kinase interaction motif or the D-motif within p38, which contains one of the redox-sensitive cysteines (Cys-119), which is separated from the other (Cys-162) by 12.7 Å (Fig. 5B). Moreover, this cysteine pair is highly conserved (Fig. 5B). The incubation of dually phosphorylated (activated) p38 with HePTP for 30 min at 30 °C resulted in a marked dephosphorylation of p38 (Fig. 5C). This effect of HePTP was perturbed by the presence of NO<sub>2</sub>-OA which resulted in a moderate preservation of the dual phospho- and phospho-Tyr-182 signals in the presence of HePTP. Therefore, our experiments with NO<sub>2</sub>-OA indicate that it is capable of inhibiting the phosphorylation of p38 by MKK3 (Fig. 5A) and also its dephosphorylation by HePTP (Fig. 5C), most likely by adducting the redox-sensitive cysteines within p38 $\alpha$ .

#### Administration of NO<sub>2</sub>-OA prevents the formation of H<sub>2</sub>O<sub>2</sub>-induced dimer in murine hearts and perturbs contractile dysfunction

To further investigate the *in vitro* observations of NO<sub>2</sub>-OA on p38 $\alpha$  (Fig. 5A), we next examined its effect in a physiologically relevant setting. In keeping with our earlier observation in rat hearts (Fig. 1D), p38 disulfide dimers formed in mouse hearts following exposure to H<sub>2</sub>O<sub>2</sub> during aerobic perfusion, an

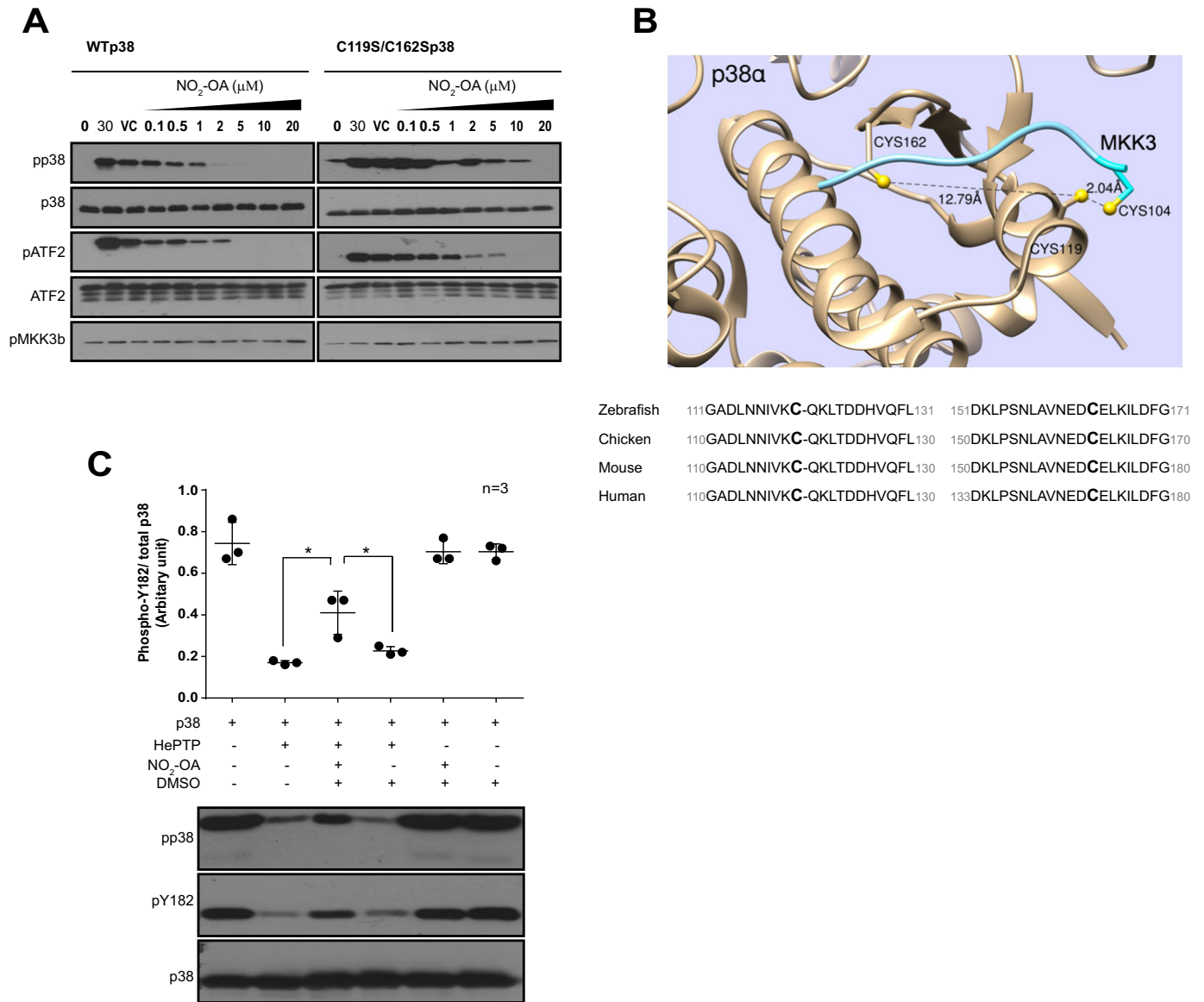


**Figure 5. Cysteine adduction attenuates activity of p38.** *A*, reducing SDS-PAGE and immunoblot analysis of WT p38 $\alpha$  and C119S/C162S p38 $\alpha$  activation by MKK3, during an *in vitro* kinase reaction in the absence or presence of 0.1–20  $\mu$ M NO<sub>2</sub>-OA, as indicated. NO<sub>2</sub>-OA adduction interferes with HePTP-mediated dephosphorylation of p38 $\alpha$ . *B*, top, ribbon representation of p38 $\alpha$ -MKK3b in complex adapted from Protein Data Bank entry 1LEZ (7). The relevant Sulfur atoms of Cys-199 and Cys-162 within p38 $\alpha$  and Cys-104 within MKK3b appear in yellow together with interatomic distances. Bottom, high conservation surrounding these regions of p38 $\alpha$ . *C*, reducing SDS-PAGE and immunoblot analysis of pre-dually phosphorylated (pTGpY) p38 $\alpha$  exposed to HePTP during an *in vitro* phosphatase reaction in the presence and absence of 25  $\mu$ M NO<sub>2</sub>-OA. The NO<sub>2</sub>-OA is solubilized in DMSO. Quantification data are shown as mean  $\pm$  S.D. (error bars). \*,  $p < 0.05$  versus NO<sub>2</sub>-OA, by one-way ANOVA and Newman-Keuls test.

effect markedly attenuated by pre-exposure to NO<sub>2</sub>-OA (Fig. 6A). Furthermore, the administration of NO<sub>2</sub>-OA resulted in a reduction of contractile dysfunction mediated by H<sub>2</sub>O<sub>2</sub> (Fig. 6, B–D), with no hearts excluded from the analysis. The detrimental effect of H<sub>2</sub>O<sub>2</sub> on cardiac performance has been extensively studied and is commonly characterized by a reduction in left ventricular developed pressure, elevation in end diastolic pressure, and increased coronary flow (18–21). Accordingly, our data showed that all of these perturbations were attenuated by pretreatment with NO<sub>2</sub>-OA (Fig. 6, B–D).

#### NO<sub>2</sub>-OA covalently modifies Cys-119 and Cys-162 of p38 $\alpha$

We next sought to determine whether NO<sub>2</sub>-OA forms a covalent adduct with p38 $\alpha$ . For this, we employed ESI-MS and

LC-MS/MS analysis using two proteases to maximize sequence coverage. We identified the residues harboring nitro-fatty acid modifications, which account for the reduced phosphorylation of p38 $\alpha$  by MKK3 (Fig. 5A) and reduced dephosphorylation by HePTP (Fig. 5C) as well as the reduced disulfide dimer formation in hearts exposed to H<sub>2</sub>O<sub>2</sub> (Fig. 6). The spectral analysis of the ESI-MS following exposure to NO<sub>2</sub>-OA (Fig. 7A) is consistent with the formation of a covalent adduct between NO<sub>2</sub>-OA and p38 $\alpha$ . Furthermore, MS/MS analysis revealed nitro-fatty acid modification of Cys-119 (Fig. 7B) and Cys-162 (Fig. 7C).

#### Discussion

Here, we demonstrate that p38 $\alpha$  has at least two redox-sensitive cysteines, 119 and 162, that lie close to a common docking

**p38 $\alpha$ -MKK3 dimerization**

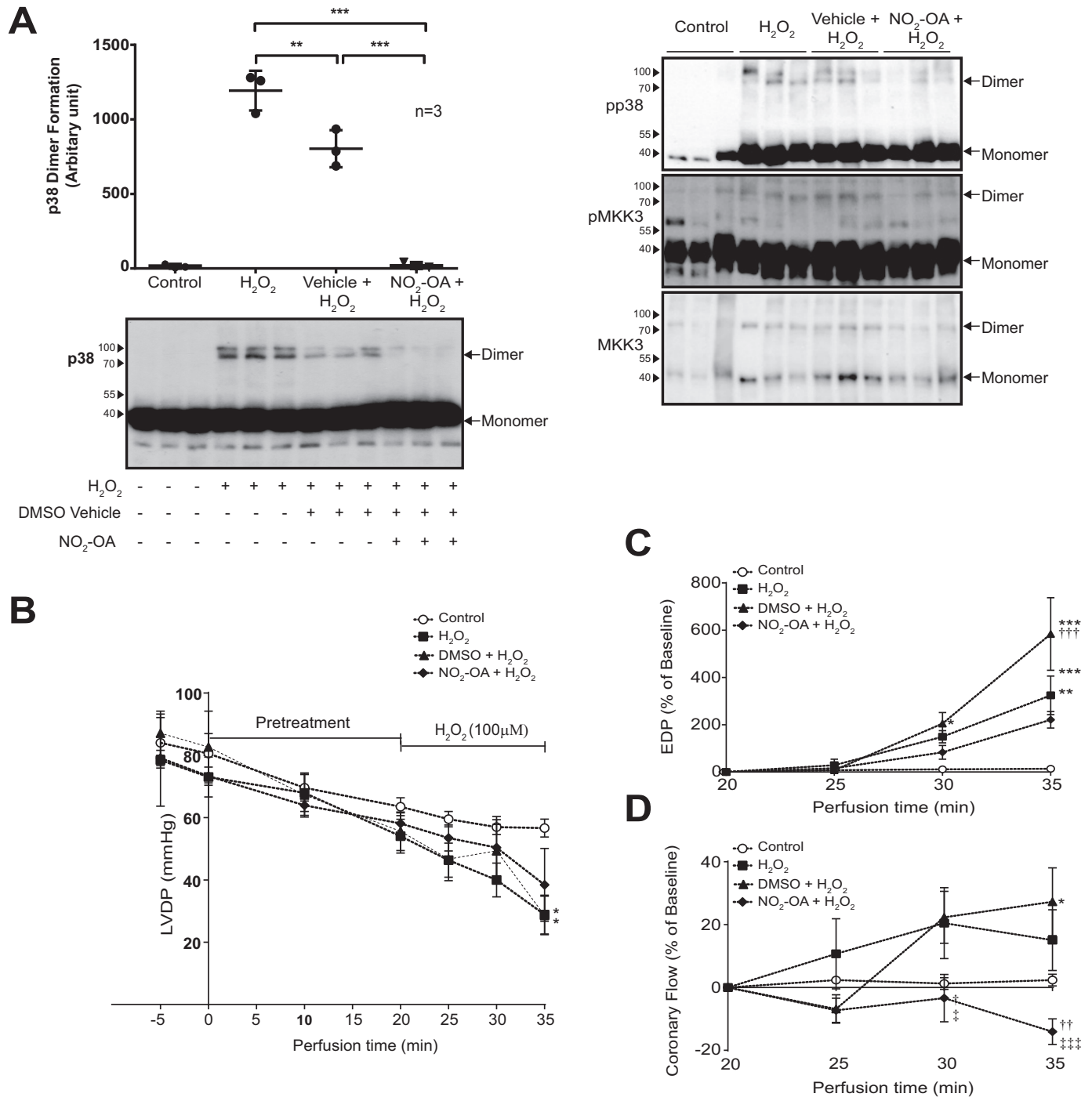


**Figure 6. Administration of NO<sub>2</sub>-OA prevents the formation of H<sub>2</sub>O<sub>2</sub>-induced dimer in murine hearts and diminishes the deleterious effect of H<sub>2</sub>O<sub>2</sub>.** A, non-reducing SDS-PAGE and immunoblot analysis of mouse hearts exposed to H<sub>2</sub>O<sub>2</sub> during aerobic Langendorff perfusion, in the absence or presence of pretreatment with 10  $\mu$ M NO<sub>2</sub>-OA in triplicate. The NO<sub>2</sub>-OA is solubilized in DMSO, which has an antioxidant effect and is present at 0.01% (v/v). p38 dimer quantification data are shown as mean  $\pm$  S.D. from three experiments. \*\*,  $p < 0.01$ ; \*\*\*,  $p < 0.001$  by one-way ANOVA followed by Tukey's test. B–D, contractile performance of mouse hearts exposed to H<sub>2</sub>O<sub>2</sub> during aerobic Langendorff perfusion, in the absence or presence of pretreatment with 10  $\mu$ M NO<sub>2</sub>-OA. Perfusion with 10  $\mu$ M NO<sub>2</sub>-OA solubilized in DMSO begins at time 0 for 20 min, and perfusion with 100  $\mu$ M H<sub>2</sub>O<sub>2</sub> begins at time 20 min for 15 min. B, left ventricular developed pressure; C, end diastolic pressure; D, coronary flow. Data are presented as mean  $\pm$  S.D. (error bars). The number of hearts per group was as follows: control, 6; H<sub>2</sub>O<sub>2</sub>, 6; H<sub>2</sub>O<sub>2</sub> in the presence of DMSO, 5; and H<sub>2</sub>O<sub>2</sub> in presence of NO<sub>2</sub>-OA, 5. \*,  $p < 0.05$  versus control; †,  $p < 0.05$  versus H<sub>2</sub>O<sub>2</sub>; ‡,  $p < 0.05$  versus H<sub>2</sub>O<sub>2</sub> in the presence of DMSO. Comparison was by two-way ANOVA with repeated measures and post hoc comparison by Bonferroni.

domain and can influence dimerization of the key upstream activator MKK3. However, disabling disulfide dimer formation by substitution of these cysteines does not seem to influence the ability of MKK3 to dually phosphorylate p38 *in vivo* or *in vitro*.

Nonetheless, when these cysteines are adducted by a biologically relevant reactive lipid, nitro-oleic acid, the binding of MKK3 and dual phosphorylation of p38 $\alpha$  are disabled. A similar effect is seen *in vitro* with the upstream deactivator, HePTP.



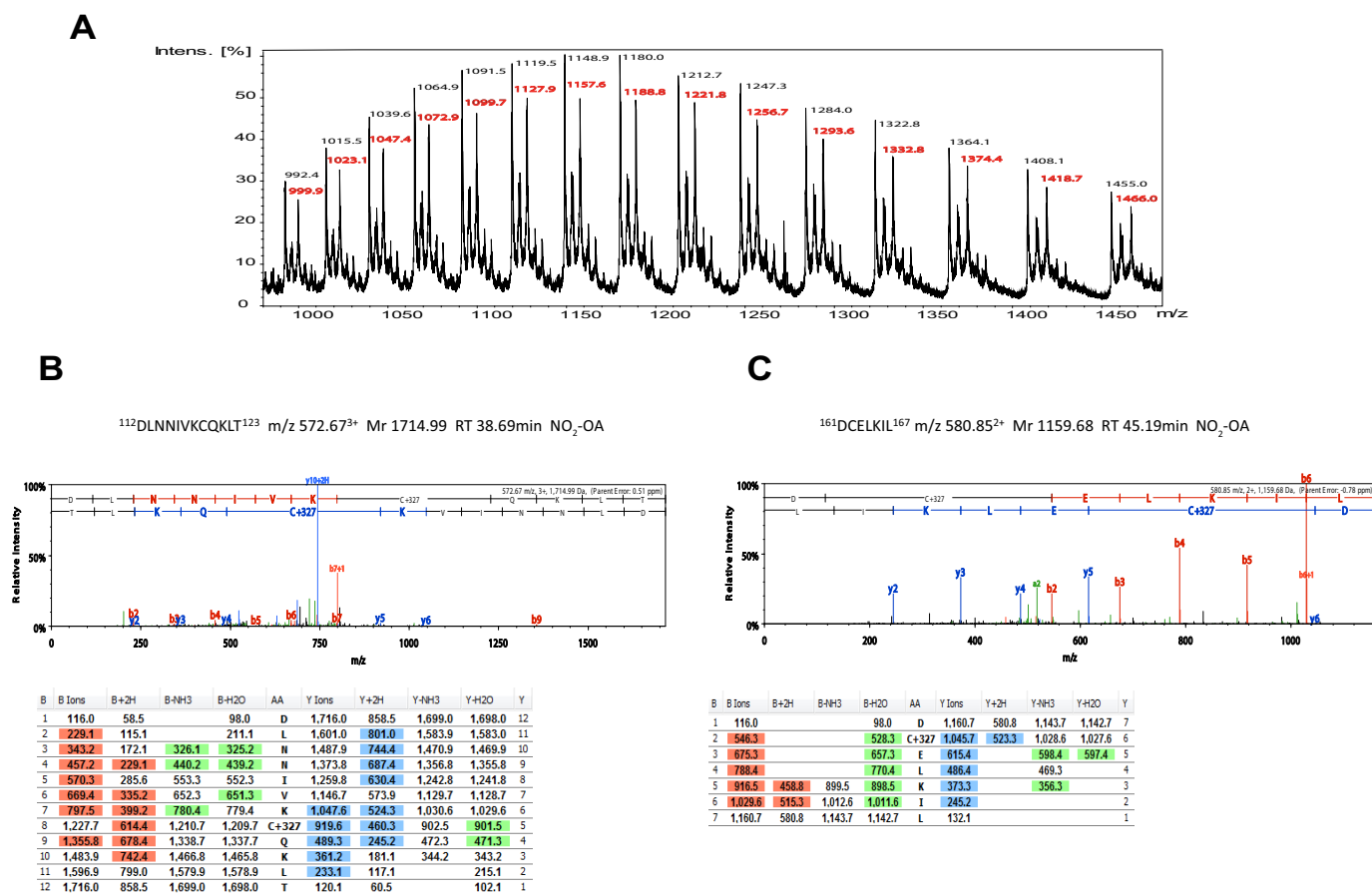


**Figure 7.  $\text{NO}_2\text{-OA}$  covalently modifies the redox-sensitive cysteines of p38 $\alpha$ .** *A*, direct infusion ESI-MS; shown in *black* is the mass of the multiple charged ion peaks belonging to non-modified p38 $\alpha$ ; shown in *boldface italic type* is the mass of the corresponding multiply charged ion peaks belonging to the  $\text{NO}_2\text{-OA}$ -modified p38 $\alpha$ . Multiply charged ion peaks belonging to mass/charge ratios from +30 to +44 for both species are shown. *B* and *C*, representative MS/MS spectra and fragmentation tables of  $\text{NO}_2\text{-OA}$ -modified peptides at Cys-119 ( $^{112}\text{DLNNIVKCQKLT}^{123}$ ) (*B*) and at Cys-162 ( $^{161}\text{DCELKIL}^{167}$ ) (*C*). *B* shows localization of a  $\text{NO}_2\text{-OA}$  modification on a peptide with  $m/z$  580.85 $^{2+}$ ; a mass difference of 430 Da (103 + 327 Da) is detected between the y5 and y6 ions. This confirms the correct assignment of the modification to Cys-162. *C* shows localization of a  $\text{NO}_2\text{-OA}$  modification on a peptide with  $m/z$  572.67 $^{3+}$ ; a mass difference of 430 Da (103 + 327 Da) is detected between the y4 and y5 ions. This confirms the correct assignment of the modification to Cys-119. The tables in *B* and *C* show *highlighted* the ions of the fragmentation profile of the peptides that are detected.

Our results add to the complexity of p38 $\alpha$  signaling, suggesting that it is not merely dependent on the balance of upstream regulatory kinases and phosphatases but that an additional level of control is exercised through redox sensors within p38 $\alpha$ .

p38 MAPK, a stress-activated kinase, is activated by divergent stimuli, including oxidative stress. It is well-known that reactive oxygen species (ROS), such as hydrogen peroxide, can induce or mediate the activation of the p38 MAPK pathway (22, 23), but the mechanisms by which ROS can activate the pathway are not well-understood. It is thought that oxidative stress is mediated by the canonical pathway of p38 $\alpha$  activation involving TAK1, a MAP3K that lies upstream of MKK3. MKK3 is known to dock on p38 $\alpha$  using the CD domain and then transphosphorylate the TGY motif to activate p38 $\alpha$ . We present here data suggesting that p38 $\alpha$  activation following exposure to  $\text{H}_2\text{O}_2$  results in the formation of a disulfide bond between p38 and MKK3. This interaction has also been alluded to by others (7, 8). We observed the formation of a disulfide dimer complex containing p38 and MKK3 following exposure to  $\text{H}_2\text{O}_2$  and with other oxidant insults. Although the disulfide dimer complex appeared to involve a small proportion of total p38 and MKK3 immunoreactivity, it was reversible upon exposure to a reduc-

ing agent ( $\beta$ -mercaptoethanol) and stabilized by auronofin, implying dynamic regulation. These observations led to the idea that the dimer was formed as a result of post-translational oxidant modification of the two proteins, p38 and MKK3. ROS are constantly generated through mitochondrial respiration and by numerous extracellular stimuli, including cytokines, growth factors, and shear stress. Under physiological conditions, they are rapidly removed by antioxidant enzymes, including superoxide dismutases, catalase, glutathione peroxidases, and peroxiredoxins, which serve to maintain a balance in the intracellular reduction-oxidation (redox) state.

One way in which ROS can alter protein structure and function is by modifying critical amino acid residues of proteins, with the thiol group of cysteine being a major target of oxidants. The oxidation of cysteine residues by  $\text{H}_2\text{O}_2$  leads to formation of the disulfide bond (-S-S-) following the generation of a sulfenyl moiety (-SOH). Sulfenates are a reversible modification, and their reversibility may represent an on-off switch allowing intricate modulation of protein activity. We verified in cells overexpressing both p38 $\alpha$  and MKK3 that the oxidant-mediated dimer formed comprised both p38 $\alpha$  and MKK3 molecules and was not a result of homodimerization by co-expression of

## p38 $\alpha$ -MKK3 dimerization

the epitope tags on both proteins. Moreover, immunoprecipitation of the FLAG-tagged p38 $\alpha$  following exposure to H<sub>2</sub>O<sub>2</sub> revealed that MKK3 indeed was complexed.

It has been previously reported that of the four cysteine residues in the human p38 $\alpha$  primary sequence, Cys-119 and Cys-162 could potentially be involved in intermolecular disulfide bond formation because they are solvent-exposed and located in flexible surface loops (24). Cys-39 and Cys-211 are buried in the molecular interior and thus not likely to be involved in oxidation phenomena. Cys-119 and Cys-162 are highly conserved in zebrafish, mouse, human, etc. and could be involved in redox regulation of p38 (Fig. 5B). As organisms have increased in complexity, the cysteine content of their constituent proteins has increased from 0.41% in Archaea to 2.26% in mammals (25). A small component of this expansion seems to relate to zinc-binding proteins or enzymes with catalytic thiols, an observation suggesting that the majority of evolutionary change relates to the acquisition of redox sensitivity. This is in keeping with our findings because Cys-119 and Cys-162 show strong evolutionary conservation (Fig. 5B). Cys-162, among many other residues, was also recently reported to be electrophilic in a large quantitative MS-based screen developed for the identification of cysteine persulfides in mammalian cells (26). Cys-109 within MKK6 was previously reported to be involved in formation of an intramolecular disulfide bond upon oxidation that inactivates MKK6 by inhibiting its ATP binding (27). Consistent with these findings, Cys-104 is the corresponding residue within MKK3 that reputedly oxidizes and forms the disulfide bond with p38 $\alpha$  in our study. Furthermore, the authors also described a pair of cysteines that could form an intramolecular disulfide bond, much akin to our observations that Cys-119 and Cys-162 acting as vicinol thiols. Collectively, these observations substantiate Cys-104 within MKK3 as having redox potential and the notion of intra- and intermolecular disulfide bonds being involved in MAP2K and MAPK activation as conceivable. The formation of the dimer was dependent on redox-sensitive cysteines, because the interaction between p38 and MKK3 was abrogated when the cysteines had been mutated to non-oxidizable serine residues. We further exploited this notion by impeding the oxidant-mediated interaction between MKK3 and p38 using the electrophilic lipid, NO<sub>2</sub>-OA, which resulted in a reduction in p38 $\alpha$  activity, which also diminished in the absence of the redox-sensitive cysteines within C119S/C162S p38.

NO<sub>2</sub>-OA, which is a component of the Mediterranean diet, has received attention due to its protective effects in murine models of hypertension (17, 28), cardiac (29), and renal (30) ischemia-reperfusion injury. Based on the crystal structure of p38 $\alpha$ , we hypothesized that NO<sub>2</sub>-OA-cysteine adduction via reversible Michael addition reactions (17) on either cysteine residue should cause steric hindrance and prevent formation of a dimer with MKK3 (see Fig. 5A). To be sure that NO<sub>2</sub>-OA could directly interact with p38 $\alpha$ , we conducted LC-MS/MS analysis and confirmed that NO<sub>2</sub>-OA indeed covalently adducted p38 $\alpha$ , specifically upon Cys-119 and Cys-162, as predicted. Our observations on the effect of NO<sub>2</sub>-OA on modulation of the p38 D-motif-interacting HePTP phosphatase and the exposure of Langendorff-perfused hearts to NO<sub>2</sub>-OA prior

to oxidant stress by H<sub>2</sub>O<sub>2</sub>, which resulted in a significant attenuation of p38 disulfide dimer formation and also the alleviation of H<sub>2</sub>O<sub>2</sub>-mediated contractile dysfunction, together complement our characterization of a novel mode of p38 regulation, not described elsewhere thus far. These observations may in part explain the anti-inflammatory effects of NO<sub>2</sub>-OA (31, 32).

The D-motif-binding site is responsible for conferring selectivity to the binding partners of p38; these include activators (MKK3), substrates (TAB1, MEF2C), and others (phosphatases). The docking strategy enables p38 to be selectively regulated by diverse signals, which must in turn also translate to specific outcomes. Our results suggest that an additional level of control is exerted by redox modification of cysteines adjacent to this binding motif that sterically control access to p38. However, although substitution of these residues abolished p38-MKK3 disulfide dimer formation, this did not seem to impact on p38 activation.

## Experimental procedures

### Adult rat ventricular myocyte culture

ARVMs were isolated from adult male Wistar rats by collagenase-based enzymatic digestion as described previously (33) and washed with M199 complete medium (M199 medium with added 100 IU/ml penicillin, 100 IU/ml streptomycin, 2 mM L-carnitine, 5 mM creatine, and 5 mM taurine). The cell suspension was allowed to settle by gravity and then resuspended in M199 complete medium and placed in laminin-coated 6-well plates before incubation in 5% CO<sub>2</sub>, room air at 37 °C. After 1 h, the medium was aspirated, leaving only adherent cells, and fresh prewarmed M199 complete medium was added. Following overnight culture, cells were exposed to the oxidant stresses, H<sub>2</sub>O<sub>2</sub> (100 and 500  $\mu$ M for 10 min), peroxynitrite (500  $\mu$ M for 30 or 60 min), SIN-1 (200  $\mu$ M for 5, 15, 30, 60, or 90 min), or diamide (50  $\mu$ M for 10 min). Cells were harvested in 2 $\times$  SDS sample buffer containing 100  $\mu$ M maleimide.

### Retrograde perfusion of isolated rodent hearts

All procedures were performed in accordance with the United Kingdom Home Office Guidance on the Operation of the Animals (Scientific Procedures) Act 1986.

Male Wistar rats (220–250 g) were anesthetized by intraperitoneal injection with sodium pentobarbital (200 mg/kg) and heparin (200 IU/kg). Hearts were rapidly excised and placed in ice-cold modified Krebs-Henseleit buffer (KHB) (118.5 mM NaCl, 25.0 mM NaHCO<sub>3</sub>, 4.75 mM KCl, 1.18 mM KH<sub>2</sub>PO<sub>4</sub>, 1.19 mM MgSO<sub>4</sub>, 11.0 mM D-glucose, and 1.4 mM CaCl<sub>2</sub>, pH 7.4). The excised hearts were cannulated via the aorta and perfused with oxygenated (95% O<sub>2</sub> and 5% CO<sub>2</sub>) KHB at 37.0 °C in a retrograde Langendorff perfusion system at a constant pressure equivalent to 72  $\pm$  1 mm Hg using a peristaltic pump and a feedback system controlled by an STH pump controller (AD Instruments, Oxford, UK). More detailed methods are described elsewhere (34). Following a 25-min stabilization, the hearts were perfused with KHB with H<sub>2</sub>O<sub>2</sub> (50, 100, 200, and 500  $\mu$ M) for 15 min.

The effect of NO<sub>2</sub>-OA on the formation of p38 dimer in hearts exposed to H<sub>2</sub>O<sub>2</sub> was examined. C57BL/6 mice (22–28 g; Harlan) were anesthetized by intraperitoneal pentobarbital

(300 mg/kg) and heparin (150 IU/kg). Hearts were rapidly excised and placed in ice-cold modified KHB. The hearts were perfused at a constant pressure of 80 mm Hg with KHB equilibrated with 95% O<sub>2</sub> and 5% CO<sub>2</sub> at 37 °C. Atrial pacing was performed ~600 beats/min. Hearts were stabilized for 30 min after the initiation of retrograde perfusion. For inclusion, all hearts had to fulfill the following criteria: time from thoracotomy to aortic cannulation < 3 min, coronary flow between 1.5 and 4 ml/min, and no persistent dysrhythmias during the stabilization period. The hearts were exposed to 10  $\mu$ M NO<sub>2</sub>-OA or vehicle control (DMSO) for 30 min prior to administration of 100  $\mu$ M H<sub>2</sub>O<sub>2</sub> for 10 min. Hearts were rapidly snap-frozen. Hearts were thawed and homogenized in extraction buffer (50 mM Tris-HCl, pH 7.5, 1 mM EDTA, 1 mM EGTA, 1 mM Na<sub>3</sub>VO<sub>4</sub>, 50 mM NaF, 5 mM sodium pyrophosphate, 1% Triton, and 1 cOmplete<sup>®</sup> protease inhibitor tablet (Roche Diagnostics)). Heart homogenates were centrifuged at 4 °C for 10 min at 13,000 r.p.m., and supernatant was resuspended in 2 $\times$  SDS buffer containing 100  $\mu$ M maleimide, boiled for 10 min, and resolved by SDS-PAGE. In a separate set of experiments, the effect of NO<sub>2</sub>-OA on the contractility of hearts exposed to H<sub>2</sub>O<sub>2</sub> was assessed. An intraventricular fluid-filled compliant balloon attached to a pressure transducer coupled to a 4S Powerlab system (AD Instruments) allowed the continuous monitoring of contractile function, left ventricular systolic and diastolic pressures and (by difference) left ventricular developed pressure and coronary flow. Hearts were exposed to 10  $\mu$ M NO<sub>2</sub>-OA or vehicle control (DMSO) for 20 min prior to administration of 100  $\mu$ M H<sub>2</sub>O<sub>2</sub> for 15 min.

### Cell culture and transfection

HEK293 and H9C2 cell lines (ATCC) were maintained in DMEM supplemented with 10% FCS and 100 IU/ml penicillin and 100 IU/ml streptomycin in 5% CO<sub>2</sub>, room air at 37 °C. Cells were cultured in 6-well plates and transfected at 70% confluence in Opti-MEM (Life Technologies) using Turbofect<sup>™</sup> reagent (Thermo Scientific) and the relevant plasmid DNAs. Wild-type p38 $\alpha$  MAPK-expressing plasmid was obtained from Jiahui Han (Scripps Research Institute, La Jolla, CA) (35). p38 $\alpha$  constructs with either Cys-119 or Cys-162 or both mutated to serine were generated by QuikChange<sup>®</sup> site-directed mutagenesis (Stratagene). MKK3 was from Par Gerwins (University of Uppsala, Uppsala, Sweden) (36). All p38 $\alpha$  constructs were FLAG-tagged, and MKK3 was hemagglutinin-tagged and cloned into the mammalian expression plasmid pcDNA3 (Invitrogen). 24 h post-transfection, cells were exposed to 100  $\mu$ M H<sub>2</sub>O<sub>2</sub> for 10 min with or without pre-exposure to 10-nitrooleic acid and harvested in 2 $\times$  SDS sample buffer containing 100  $\mu$ M maleimide.

### Co-immunoprecipitation

Cells were washed in ice-cold PBS and lysed in 400  $\mu$ l of iced lysis buffer (50 mM Tris-HCl, pH 7.4, 150 mM NaCl, mM EDTA, 1% Triton X-100, one protease inhibitor mixture tablet per 50 ml (cOmplete<sup>®</sup>, Roche Diagnostics)). The cells were scraped and collected into cooled microcentrifuge tubes. Cell lysates were centrifuged at 12,000  $\times$  g for 10 min at 4 °C. Supernatants were transferred into chilled tubes containing 40  $\mu$ l of a 50%

anti-FLAG M2 affinity gel slurry (Sigma), prepared as per the manufacturer's instructions. Following overnight incubation on a rotation wheel, at 4 °C, samples were centrifuged at 6,000  $\times$  g for 30 s to pellet the anti-FLAG M2 affinity gel-bound proteins, followed by three washes with 0.5 ml of lysis buffer. Samples were resuspended in 2 $\times$  SDS sample buffer containing 100  $\mu$ M maleimide.

### Immunoblot analysis

Samples were resolved on a 10% SDS-polyacrylamide gel under non-reducing conditions and transferred onto PVDF membranes. After blocking in 4% nonfat milk and 1% BSA in Tris-buffered saline, pH 7.4, for 1 h, membranes were exposed to the following primary antibodies: anti-dual phospho-p38 MAPK (Thr-180 and Tyr-182; 9211, Cell Signaling), anti-p38 MAPK (9212, Cell Signaling), anti-phospho MEK3 (ab131283, Abcam), MEK3 (ab47522, Abcam), anti-phospho ATF-2 (9221, Cell Signaling), anti-ATF-2 (9226, Cell Signaling), anti-HA (2367, Cell Signaling), or anti-FLAG (2368, Cell Signaling) all at 1:1,000 overnight at 4 °C with agitation. After washing and incubation with HRP-conjugated secondary antibody (1:2,000) (NA934V, GE Healthcare), antigen-antibody complexes were visualized by enhanced chemiluminescence detection (Pierce).

### Expression and purification of WT p38 $\alpha$ , p38 $\alpha$ C119S, p38 $\alpha$ C162S, and p38 $\alpha$ C119S/C162S recombinant proteins

DNA encoding p38 $\alpha$  was derived from a pET14b vector kindly donated by Y. Wang (37) and subcloned into a pET-Duet-1 vector. The full coding sequence included an N-terminal His<sub>6</sub> tag followed by a tobacco etch virus cleavage site and mouse p38 $\alpha$ . The p38 $\alpha$  mutants were generated by overlapping C and N terminus fragments produced by PCR with complementary internal primers containing the desired mutations. The PCR products were then combined to form the template for a second PCR with external primers. The vectors were transformed in *E. coli* strain Rosetta II cells (Novagen). The protein expression and purification procedure followed was as described previously (38). Following dialysis overnight at 4 °C in 100 mM NaCl, 20 mM Tris, and 5 mM TCEP (Invitrogen) (pH 7.5), purified proteins were aliquoted and stored at -80 °C.

### Vicinal thiol analysis of p38 $\alpha$

The formation of an intramolecular disulfide bond between Cys-119 and Cys-162 in p38 $\alpha$  was measured using dBB. dBB is a fluorogenic homobifunctional thiol-specific cross-linking reagent that is non-fluorescent until both of its alkylating groups have been reacted by vicinal thiols. It then emits light, which can be measured at 477 nm.

75  $\mu$ g of recombinant wild-type p38 $\alpha$  (WT p38 $\alpha$ ) was transferred into a cooled tube containing 100 mM Tris buffer (pH 7.4) and reduced by the addition of TCEP (Invitrogen) to a final concentration of 5 mM for 15 min at room temperature. The TCEP concentration was further diluted to 50  $\mu$ M by the addition of 100 mM Tris buffer (pH 7.4). 2.5  $\mu$ g (w/v) of the reduced protein was then transferred to a well of a black 96-well plate (Sterilin, ThermoFisher Scientific) containing either 100 mM Tris buffer (pH 7.4) alone or with 500  $\mu$ M H<sub>2</sub>O<sub>2</sub> or 1 mM diamide and incubated for 15 min at room temperature. Finally,

## p38 $\alpha$ -MKK3 dimerization

100  $\mu$ M dBBr (Invitrogen) was added, and samples were incubated at room temperature for 15 min in the dark before monitoring fluorescence in a plate reader with fluorescence excitation/emission spectra of 385/477 nm.

TCEP was removed from 75  $\mu$ g of recombinant WT p38 $\alpha$ , C119S p38 $\alpha$ , or C119S/C162S p38 $\alpha$  using 7,000 molecular weight cut-off Zeba<sup>TM</sup> spin desalting columns (Thermo Scientific) as per the manufacturer's instructions. 2.5  $\mu$ g (w/v) of the desalted protein sample was immediately transferred to the wells of a 96-well plate containing 100 mM Tris buffer (pH 7.4) and 100  $\mu$ M dBBr and incubated at room temperature for 15 min in the dark before monitoring fluorescence in a plate reader with fluorescence excitation/emission spectra of 385/477 nm.

### Simulated ischemia/reperfusion protocol

Simulated ischemia was induced by exposing H9c2 cells cultured on 6-well plates for the specified duration to modified KHB (137 mM NaCl, 3.58 mM KCl, 0.49 mM MgCl<sub>2</sub>, 1.8 mM CaCl<sub>2</sub>, and 4.0 mM HEPES) with 20 mM 2-deoxyglucose, 20 mM sodium lactate, and 1 mM sodium dithionite at pH 6.5 in 5% CO<sub>2</sub>, room air at 37 °C (13). The buffer was aspirated, and then cells were either collected in 2 $\times$  SDS sample buffer containing 100  $\mu$ M maleimide or reperfused by the addition of serum-free DMEM for the specified duration before collecting in 2 $\times$  SDS sample buffer containing 100  $\mu$ M maleimide.

### In vitro kinase assay

The effect of the endogenous electrophilic lipid, NO<sub>2</sub>-OA, on the activation and activity of p38 *in vitro* was examined. Purified recombinant p38 $\alpha$  (0.1  $\mu$ M) was incubated with NO<sub>2</sub>-OA (10037, Cayman Chemical) in buffer containing 100 mM NaCl, 20 mM Tris, pH 7.5, 2 mM MgCl, and 200  $\mu$ M ATP at 37 °C for 30 min. The reaction, in a 50- $\mu$ l final volume, was started by the addition of 0.1  $\mu$ g of MKK3b, 0.5  $\mu$ g of ATF-2 fusion protein (9224, Cell Signaling) and incubated at 30 °C for 30 min. The reaction was stopped by the addition of 5 $\times$  SDS sample buffer, and samples were resolved by SDS-PAGE and transferred onto PVDF membranes.

The effect of NO<sub>2</sub>-OA on the ability of HePTP to dephosphorylate p38 $\alpha$  was examined. Purified recombinant activated dually phosphorylated p38 $\alpha$  (3  $\mu$ M) was prepared as described previously (34) and incubated with NO<sub>2</sub>-OA (15  $\mu$ M) in buffer containing 5 mM MOPS, 10 mM NaCl, 10  $\mu$ M EDTA, pH 7.0, at 37 °C for 30 min. The reaction, in a 40- $\mu$ l final volume, was started by the addition of 0.3  $\mu$ M purified recombinant HePTP, prepared and purified from a plasmid vector kindly donated by W. Peti (39) and incubated at 30 °C for 30 min. The reaction was stopped by the addition of 5 $\times$  SDS sample buffer, and samples were resolved by SDS-PAGE.

### Liquid chromatography tandem mass spectrometry (LC-MS/MS) analysis

ESI-MS and LC-MS/MS were carried out to determine whether NO<sub>2</sub>-OA forms a covalent adduct with p38 $\alpha$ . p38 $\alpha$  at 1 mg/ml was treated with equimolar 10 nitro-oleic acid at room temperature for 1 h. The reaction mixture was then analyzed by direct-infusion ESI-MS and LC-MS/MS. To improve sequence

coverage with LC-MS/MS, both trypsin and Asp-N were used to digest p38 $\alpha$ .

For enzymatic digestion, in-solution reduction, alkylation, and digestion with trypsin or Asp-N of total p38 $\alpha$  protein was performed prior to subsequent analysis by mass spectrometry by following methods described previously (40). Briefly, cysteine residues were reduced with TCEP, because the NO<sub>2</sub>-OA modification adduct is not stable in the presence of dithiothreitol, and derivatized by treatment with iodoacetamide to form stable carbamidomethyl derivatives. Trypsin and Asp-N digestion was carried out for 16 h at 37 °C.

### LC-MS/MS

Chromatographic separations were performed using an EASY NanoLC system (ThermoFisher Scientific). Peptides from a total protein amount of 2 mg on column were resolved by reversed phase chromatography on a 75- $\mu$ m C18 column using a three-step linear gradient of acetonitrile in 0.1% formic acid. The gradient was delivered to elute peptides at a flow rate of 300 nl/min over 60 min. The eluate was ionized by electrospray ionization using an Orbitrap Velos Pro (ThermoFisher Scientific), operating under Xcalibur version 2.2. The instrument was programmed to acquire in automated data-dependent switching mode, selecting precursor ions based on their intensity for sequencing by collision-induced fragmentation using a Top20 collision-induced dissociation method. The MS/MS analyses were conducted using collision energy profiles that were chosen based on the mass-to-charge ratio (*m/z*) and the charge state of the peptide.

*Author contributions*—M. S. M. conceived and coordinated the study and wrote the paper. R. B. wrote the paper and designed, performed, and analyzed the experiments shown in Figs. 1–6. J. R. B. and P. E. provided intellectual and technical assistance throughout and contributed to final revisions of the manuscript. G. F. D. designed, performed, and analyzed the experiments shown in Fig. 7. O. R. performed the experiments shown in Fig. 1D. V. D. performed the experiment shown in Fig. 5C. R. L. C. provided technical assistance with the design of the experiments shown in Fig. 4. All authors reviewed the final version of the manuscript.

### References

1. English, J., Pearson, G., Wilsbacher, J., Swantek, J., Karandikar, M., Xu, S., and Cobb, M. H. (1999) New insights into the control of MAP kinase pathways. *Exp. Cell Res.* **253**, 255–270
2. Ashwell, J. D. (2006) The many paths to p38 mitogen-activated protein kinase activation in the immune system. *Nat. Rev. Immunol.* **6**, 532–540
3. Martin, E. D., Bassi, R., and Marber, M. S. (2015) p38 MAPK in cardioprotection: are we there yet? *Br. J. Pharmacol.* **172**, 2101–2113
4. Akella, R., Moon, T. M., and Goldsmith, E. J. (2008) Unique MAP kinase binding sites. *Biochim. Biophys. Acta* **1784**, 48–55
5. Tanoue, T., Adachi, M., Moriguchi, T., and Nishida, E. (2000) A conserved docking motif in MAP kinases common to substrates, activators and regulators. *Nat. Cell Biol.* **2**, 110–116
6. Zhou, T., Sun, L., Humphreys, J., and Goldsmith, E. J. (2006) Docking interactions induce exposure of activation loop in the MAP kinase ERK2. *Structure* **14**, 1011–1019
7. Chang, C. I., Xu, B. E., Akella, R., Cobb, M. H., and Goldsmith, E. J. (2002) Crystal structures of MAP kinase p38 complexed to the docking sites on its nuclear substrate MEF2A and activator MKK3b. *Mol. Cell* **9**, 1241–1249

8. Akella, R., Min, X., Wu, Q., Gardner, K. H., and Goldsmith, E. J. (2010) The third conformation of p38 $\alpha$  MAP kinase observed in phosphorylated p38 $\alpha$  and in solution. *Structure* **18**, 1571–1578
9. Dröge, W. (2002) Free radicals in the physiological control of cell function. *Physiol. Rev.* **82**, 47–95
10. Burgoyne, J. R., and Eaton, P. (2011) Contemporary techniques for detecting and identifying proteins susceptible to reversible thiol oxidation. *Biochem. Soc. Trans.* **39**, 1260–1267
11. Spadaro, D., Yun, B. W., Spoel, S. H., Chu, C., Wang, Y. Q., and Loake, G. J. (2010) The redox switch: dynamic regulation of protein function by cysteine modifications. *Physiol. Plant* **138**, 360–371
12. Sanchez, R., Riddle, M., Woo, J., and Momand, J. (2008) Prediction of reversibly oxidized protein cysteine thiols using protein structure properties. *Protein Sci.* **17**, 473–481
13. Pun, A., Mockridge, J. W., Farooqui, S., Marber, M. S., and Heads, R. J. (2000) Sustained activation of p42/p44 mitogen-activated protein kinase during recovery from simulated ischaemia mediates adaptive cytoprotection in cardiomyocytes. *Biochem. J.* **350**, 891–899
14. Saurin, A. T., Martin, J. L., Heads, R. J., Foley, C., Mockridge, J. W., Wright, M. J., Wang, Y., Marber, M. S. (2000) The role of differential activation of p38-mitogen-activated protein kinase in preconditioned ventricular myocytes. *FASEB J.* **14**, 2237–2246
15. Mockridge, J. W., Marber, M. S., and Heads, R. J. (2000) Activation of Akt during simulated ischemia/reperfusion in cardiac myocytes. *Biochem. Biophys. Res. Commun.* **270**, 947–952
16. Engelbrecht, A. M., Niesler, C., Page, C., and Lochner, A. (2004) p38 and JNK have distinct regulatory functions on the development of apoptosis during simulated ischaemia and reperfusion in neonatal cardiomyocytes. *Basic Res. Cardiol.* **99**, 338–350
17. Charles, R. L., Rudyk, O., Prysazhna, O., Kamynina, A., Yang, J., Morisseau, C., Hammock, B. D., Freeman, B. A., and Eaton, P. (2014) Protection from hypertension in mice by the Mediterranean diet is mediated by nitro fatty acid inhibition of soluble epoxide hydrolase. *Proc. Natl. Acad. Sci. U.S.A.* **111**, 8167–8172
18. Shattock, M. J., Manning, A. S., and Hearse, D. J. (1982) Effects of hydrogen peroxide on cardiac function and post-ischaemic functional recovery in the isolated “working” rat heart. *Pharmacology* **24**, 118–122
19. Zimmer, K. M., and Karmazyn, M. (1997) Prostaglandins attenuate cardiac contractile dysfunction produced by free radical generation but not by hydrogen peroxide. *Mol. Cell. Biochem.* **176**, 171–178
20. Meldrum, D. R., Dinarello, C. A., Cleveland, J., Cain, B. S., Shames, B. D., Meng, X., and Harken, A. H. (1998) Hydrogen peroxide induces tumor necrosis factor  $\alpha$ -mediated cardiac injury by a P38 mitogen-activated protein kinase-dependent mechanism. *Surgery* **124**, 291–297
21. Matsumoto, Y., Kaneko, M., Iimuro, M., Fujise, Y., and Hayashi, H. (2000) Role of high-energy phosphate metabolism in hydrogen peroxide-induced cardiac dysfunction. *Mol. Cell. Biochem.* **204**, 97–106
22. Gutiérrez-Uzquiza, Á., Arechederra, M., Bragado, P., Aguirre-Ghiso, J. A., and Porras, A. (2012) p38 $\alpha$  mediates cell survival in response to oxidative stress via induction of antioxidant genes: effect on the p70S6K pathway. *J. Biol. Chem.* **287**, 2632–2642
23. Yamada, T., Egashira, N., Bando, A., Nishime, Y., Tonogai, Y., Imuta, M., Yano, T., and Oishi, R. (2012) Activation of p38 MAPK by oxidative stress underlying epirubicin-induced vascular endothelial cell injury. *Free Radic. Biol. Med.* **52**, 1285–1293
24. Patel, S. B., Cameron, P. M., Frantz-Wattley, B., O'Neill, E., Becker, J. W., and Scapin, G. (2004) Lattice stabilization and enhanced diffraction in human p38 $\alpha$  crystals by protein engineering. *Biochim. Biophys. Acta* **1696**, 67–73
25. Miseta, A., and Csutora, P. (2000) Relationship between the occurrence of cysteine in proteins and the complexity of organisms. *Mol. Biol. Evol.* **17**, 1232–1239
26. Longen, S., Richter, F., Köhler, Y., Wittig, I., Beck, K. F., and Pfeilschifter, J. (2016) Quantitative persulfide site identification (qPerS-SID) reveals protein targets of H<sub>2</sub>S releasing donors in mammalian cells. *Sci. Rep.* **6**, 29808
27. Diao, Y., Liu, W., Wong, C. C., Wang, X., Lee, K., Cheung, P. Y., Pan, L., Xu, T., Han, J., Yates, J. R., 3rd, Zhang, M., and Wu, Z. (2010) Oxidation-induced intramolecular disulfide bond inactivates mitogen-activated protein kinase kinase 6 by inhibiting ATP binding. *Proc. Natl. Acad. Sci. U.S.A.* **107**, 20974–20979
28. Klinke, A., Möller, A., Pekarova, M., Ravekes, T., Friedrichs, K., Berlin, M., Scheu, K. M., Kubala, L., Kolarova, H., Ambrozova, G., Schermuly, R. T., Woodcock, S. R., Freeman, B. A., Rosenkranz, S., Baldus, S., Rudolph, V., and Rudolph, T. K. (2014) Protective effects of 10-nitro-oleic acid in a hypoxia-induced murine model of pulmonary hypertension. *Am. J. Respir. Cell Mol. Biol.* **51**, 155–162
29. Rudolph, V., Rudolph, T. K., Schopfer, F. J., Bonacci, G., Woodcock, S. R., Cole, M. P., Baker, P. R. S., Ramani, R., and Freeman, B. A. (2010) Endogenous generation and protective effects of nitro-fatty acids in a murine model of focal cardiac ischaemia and reperfusion. *Cardiovasc. Res.* **85**, 155–166
30. Liu, H., Jia, Z., Soodvilai, S., Guan, G., Wang, M. H., Dong, Z., Symons, J. D., and Yang, T. (2008) Nitro-oleic acid protects the mouse kidney from ischemia and reperfusion injury. *Am. J. Physiol. Renal Physiol.* **295**, F942–F949
31. Groeger, A. L., and Freeman, B. A. (2010) Signaling actions of electrophiles: anti-inflammatory therapeutic candidates. *Mol. Interv.* **10**, 39–50
32. Cui, T., Schopfer, F. J., Zhang, J., Chen, K., Ichikawa, T., Baker, P. R. S., Batthyany, C., Chacko, B. K., Feng, X., Patel, R. P., Agarwal, A., Freeman, B. A., and Chen, Y. E. (2006) Nitrated fatty acids: endogenous anti-inflammatory signaling mediators. *J. Biol. Chem.* **281**, 35686–35698
33. Bellahcene, M., Jacquet, S., Cao, X. B., Tanno, M., Haworth, R. S., Layland, J., Kabir, A. M., Gaestel, M., Davis, R. J., Flavell, R. A., Shah, A. M., Avkiran, M., and Marber, M. S. (2006) Activation of p38 mitogen-activated protein kinase contributes to the early cardiodepressant action of tumor necrosis factor. *J. Am. Coll. Cardiol.* **48**, 545–555
34. DeNicola, G. F., Martin, E. D., Chaikuad, A., Bassi, R., Clark, J., Martino, L., Verma, S., Sicard, P., Tata, R., Atkinson, R. A., Knapp, S., Conte, M. R., and Marber, M. S. (2013) Mechanism and consequence of the autoactivation of p38 $\alpha$  mitogen-activated protein kinase promoted by TAB1. *Nat. Struct. Mol. Biol.* **20**, 1182–1190
35. Ge, B., Gram, H., Di Padova, F., Huang, B., New, L., Ulevitch, R. J., Luo, Y., and Han, J. (2002) MAPKK-independent activation of p38 $\alpha$  mediated by TAB1-dependent autophosphorylation of p38 $\alpha$ . *Science* **295**, 1291–1294
36. Matsumoto, T., Turesson, I., Book, M., Gerwins, P., and Claesson-Welsh, L. (2002) p38 MAP kinase negatively regulates endothelial cell survival, proliferation, and differentiation in FGF-2-stimulated angiogenesis. *J. Cell Biol.* **156**, 149–160
37. Wang, Y., Huang, S., Sah, V. P., Ross, J., Jr., Brown, J. H., Han, J., and Chien, K. R. (1998) Cardiac muscle cell hypertrophy and apoptosis induced by distinct members of the p38 mitogen-activated protein kinase family. *J. Biol. Chem.* **273**, 2161–2168
38. Bukhtiyarova, M., Northrop, K., Chai, X., Casper, D., Karpusas, M., and Springman, E. (2004) Improved expression, purification, and crystallization of p38 $\alpha$  MAP kinase. *Protein Expr. Purif.* **37**, 154–161
39. Francis, D. M., Różycki, B., Koveal, D., Hummer, G., Page, R., and Peti, W. (2011) Structural basis of p38 $\alpha$  regulation by hematopoietic tyrosine phosphatase. *Nat. Chem. Biol.* **7**, 916–924
40. Kansanen, E., Bonacci, G., Schopfer, F. J., Kuosmanen, S. M., Tong, K. I., Leinonen, H., Woodcock, S. R., Yamamoto, M., Carlberg, C., Ylä-Herttuala, S., Freeman, B. A., and Levenon, A. L. (2011) Electrophilic nitro-fatty acids activate NRF2 by a KEAP1 cysteine 151-independent mechanism. *J. Biol. Chem.* **286**, 14019–14027